J. Membrane Biol. 49, 325–344 (1979)

Zinc-Dependent Action Potentials in Giant Neurons of the Snail, *Euhadra quaestia*

Kazuyoshi Kawa*

Department of Physiology, Faculty of Medicine, University of Tokyo, Bunkyo-ku, Tokyo, Japan

Received 13 March 1979; revised 1 June 1979

Summary. In giant neurons of subesophageal ganglion of the Japanese land snail, *Euhadra quaestia* Deshayes, permeation of Zn ions through Ca channels were investigated with a conventional current clamp method.

All-or-none action potentials of long duration (90 to 120 sec) were evoked in 24 mM Zn containing salines. The overshoots were about +10 mV and the maximum rate of rises (MRRs) was about 2.9 V/sec. The amplitudes and the MRRs of the action potentials depended on external Zn ion concentrations.

The action potentials were suppressed by specific Ca-channel inhibitors such as Co^{2+}, La^{3+} and Verapamil, but they were resistant to Na-channel inhibitor, tetrodotoxin, even at 30 μM.

It is concluded that these action potentials are generated by Zn ions permeating Ca channels in snail neuronal membrane.

On the basis of Hagiwara and Takahashi's (S. Hagiwara & K. Takahashi, 1967, *J. Gen. Physiol.* **50**:583) model of Ca channels, it is inferred that Zn ions are 5 to 10 times stronger in affinity to Ca channels than Ca ions, but 10 to 20 times less permeable.

The Zn ion has been considered as a competitive inhibitor of Ca channels in excitable membranes. This applies not only to invertebrate muscle membrane (Hagiwara & Takahashi, 1967) but also to presynaptic nerve terminals because Ca ions entering nerve terminals at excitation trigger transmitter releases (Katz & Miledi, 1965), the amount of which is decreased by external Zn ions (Sandow & Bien, 1962; Miledi, 1966; Benoit & Mambrini, 1970).

Recently, Fukuda and Kawa (1977) have reported that in skeletal muscles of insect larvae Zn ions can permeate Ca channels in the muscle membrane. One may wonder, however, if this Zn permeability is specific to an immature membrane at a larval stage (*see* Belton & Grundfest, 1962; Kusano & Grundfest, 1967), but not to adult ones.

* *Present address:* Department of Pharmacology, School of Medicine, Gunma University, Showa-machi, Maebashi, Japan.

0022-2631/79/0049-0325 $04.00

The present study was carried out to examine whether permeation of Zn ions through Ca channels also occurs in Ca channels of mature molluscan giant neurons. Molluscan neurons generate both Na- and Ca-dependent action potentials (Kerkut & Gardner, 1967; Wald, 1972; Standen, 1975*a*) by ionic permeation through associated Na and Ca channels, respectively (Standen, 1975*b*; Kostyuk & Krishtal, 1977*a*; Akaike, Lee & Brown, 1978). And these Ca channels are considered as handy analogues of those at the synaptic nerve terminals (Klein & Kandel, 1978). It was demonstrated that Zn ions permeate Ca channels of mature molluscan neurons and thereby generate an all-or-none action potential.

Materials and Methods

Preparation

Japanese land snails, *Euhadra quaestia* Deshayes, were collected in gardens and raised in an artificial environment. They subsist for more than one year on sweet potatoes.

The subesophageal ganglion was dissected from the adult snail (10 to 15 g) with its associated nerves and pinned, dorsal surface upward, on a fluorocarbon-polymer base in a Lucite chamber. Under binocular microscope ($\times 60$), connective tissues covering the group of giant neurons were removed with watchmaker's forceps. The thin inner connective tissues were also removed carefully.

I identified two giant neurons (about 200 μm in diameter) for this study which were located on the caudal end of the ganglion just between the intestinal nerve and the anal nerve. These two cells showed no significant differences in regard to this study. They correspond to the cells named *1* and *2* in the subesophageal ganglion of *Euhadra peliomphala* (Sugaya, Sugaya & Tsujitani, 1973).

Electrical Recordings

Under binocular microscope, two glass microelectrodes filled with 3 M KCl were introduced into an identified neurone; one (10 to 15 MΩ) was used for recording the intracellular potential and the other (8 to 10 MΩ) for intracellular injection of currents.

Both electrodes were connected to FET-input preamplifiers (made of Teledyne 1026) via chloride-coated silver wire. One preamplifier was equipped with a bootstrap circuit for current injection where 100 MΩ resistor was connected to the head of the preamplifier (Miyazaki, Ohmori & Sasaki, 1975).

An indifferent electrode in the chamber was connected to virtually grounded input of an operational amplifier (feedback resistor of 1 MΩ; Teledyne 1026) via chloride-coated silver wire. The current passed through the membrane was measured as a return current from the indifferent electrode.

The intracellular potential was further differentiated with an electronic circuit to obtain the rate of change in the membrane potential. Especially, the maximum rate of rise (MRR) of an action potential was considered as nearly proportional to the maximum inward current during the genesis of the action potential (Ferroni & Blanchi, 1965). The circuit

for differentiation operated linearly as long as the rate of change in the membrane potential did not exceed 100 V/sec.

The outputs of the amplifiers were connected to an oscilloscope (Iwatsu Electric Co., Ltd. SS-5201) and displayed. The membrane potential was also monitored with a pen-recorder (TOA Electronics Ltd. EPR-2TB).

Extracellular Solutions

The subesophageal ganglion was prepared in standard snail saline, whose ionic composition was the same as Kerkut and Gardner (1967) as shown in Table 1 together with other experimental salines. In the experimental salines, NaCl was replaced by equimolar TrisCl. When concentrations of divalent cations were altered, the concentration of TrisCl was also changed so as to keep the osmolarity constant. Difference of activity coefficients between monovalent cations and divalent cations were neglected, as this would introduce an error of less than 3%.

When the extracellular Ca ion concentration was made low, the preparation was perfused beforehand with $MgCl_2$ 24 saline (which contains 24 mM $MgCl_2$; No. 2 saline in Table 1) for more than 30 min for washing out remaining Ca ions and further with EGTA 10 saline (No. 4 in Table 1) for 4 to 8 min for chelating extracellular Ca ions. In the

Table 1. Composition of salines (mM)

No.	Saline name	KCl	$CaCl_2$	$MgCl_2$	$ZnCl_2$	TrisCl	Other ions
1	Standard[a]	4	7	5	(−)	5	NaCl 80
2	$MgCl_2$ 24	4	(−)	24	(−)	67	(−)
3	$ZnCl_2$ 24	4	(−)	(−)	24	67	(−)
4	EGTA 10[b]	4	(−)	24	(−)	52	EGTA 10
5	$CaCl_2$ 10	4	10	(−)	(−)	88	(−)
6	Ca 10 Zn 3	4	10	(−)	3	83.5	(−)
7	Ca 10 Zn 6	4	10	(−)	6	79	(−)
8	Ca 10 Zn 12	4	10	(−)	12	70	(−)
9	Ca 10 Zn 24	4	10	(−)	24	52	(−)

Fluoride salines

No.	Saline name	KF	TEACl	ZnF_2	TrisCl	Other ions
10	ZnF_2 24	4	(−)	24	67	(−)
11	ZnF_2 3 TEA	4	50	3	35.7	PIPES 10[c]
12	ZnF_2 6 TEA	4	50	6	31.2	PIPES 10[c]
13	ZnF_2 12 TEA	4	50	12	22.2	PIPES 10[c]
14	ZnF_2 24 TEA	4	50	24	4.2	PIPES 10[c]
15	ZnF_2 24 Co10	4	(−)	24	52	$CoCl_2$ 10

[a] pH 7.4; all the other salines are adjusted to pH 6.9 as mentioned in the text.

[b] pH of this saline was continuously monitored by the color of added phenol red (0.01%). EGTA is neutralized by adding Tris-OH.

[c] pH of PIPES (pKa_2, 6.8) is adjusted to 6.9 by Tris-OH.

presence of Zn ions, however, EGTA (ethylene glycol bis (β-aminoethyl ether)-N, N, N′, N′,-tetraacetic acid) cannot be used for buffering Ca ion concentration, because EGTA has a higher affinity with Zn ions than Ca ions. Therefore, fluoride ions instead of EGTA were used for buffering the Ca ion concentration (fluoride salines in Table 1). As the solubility product of CaF_2 is very low (2.7×10^{-11}; Dean, 1973), Ca ion concentration in these salines was estimated as low as 10^{-8} M.

The pH of all the experimental salines were adjusted to 6.9 because of the solubility limitation of Zn ions. At pH 6.9, Zn ions up to 24 mM could be solved stably; neither precipitate nor change in pH were detected even after a week (*see* methods of Murayama & Lakshminarayanaiah, 1977). At pH 6.9, the buffer action of TrisCl is weak, because 96% of the toal TrisCl is dissociated at this pH. Therefore in salines containing less than 50 mM TrisCl (No. 11 to 14 salines in Table 1), 10 mM PIPES (piperazine-N, N′,-bis (2-ethanesulphonic acid)-Tris was added as buffer.

In some experiments, tetrodotoxin (TTX; 30 μM; Sankyo, Japan) or Verapamil (10^{-5} to 10^{-4} g/ml; Eisai, Japan) was added to salines in Table 1. The potency of TTX was checked on frog sciatic nerve preparations. The volume of the chamber was about 1.2 ml and when I changed the extracellular saline, I perfused the chamber with a new saline of 25 ml at a rate of 3 ml/min. Such rate of saline change was shown to be adequate by observing the removal of methylene blue solution from the chamber. Experiments were performed at room temperature (23–28 °C).

Results

Action Potentials in Zn Saline

In standard snail saline, giant neurons of the snail generate both Na- and Ca-dependent action potentials (Kerkut & Gardner, 1967; Wald, 1972; Standen, 1975*a*). When Na ions were replaced with $Tris^+$, and Ca ions also with Mg (No. 2 saline in Table 1), the cell maintained resting membrane potentials of −59.4 mV (SD, 4.0 mV; $n=7$), but they generated no action potentials even with a depolarizing stimulus up to −20 mV. The membrane resistance measured by passage of small hyperpolarizing pulses (1.4 nA, 900 msec) was 4.8 MΩ on the average (SD, 0.2 MΩ, $n=4$).

However, when Mg ions were further replaced with Zn ions, all-or-none action potentials were elicited (Fig. 1), whereas the resting membrane potential was not appreciably altered, the average values being −62.5 mV (SD, 3.0 mV; $n=4$). In Fig. 1 a long lasting action potential was evoked by passage of 2.8 nA depolarizing stimulus (arrow at *a*). The membrane potential at the peak of the action potential was +11 mV and the input resistance at the plateau was less than 1/10 of that at the resting state. Such action potentials lasted for 90 to 120 sec. In the case of Fig. 1, the action potential was abolished halfway by application of a hyperpolarizing pulse (14 nA, 900 msec, arrow at *b*).

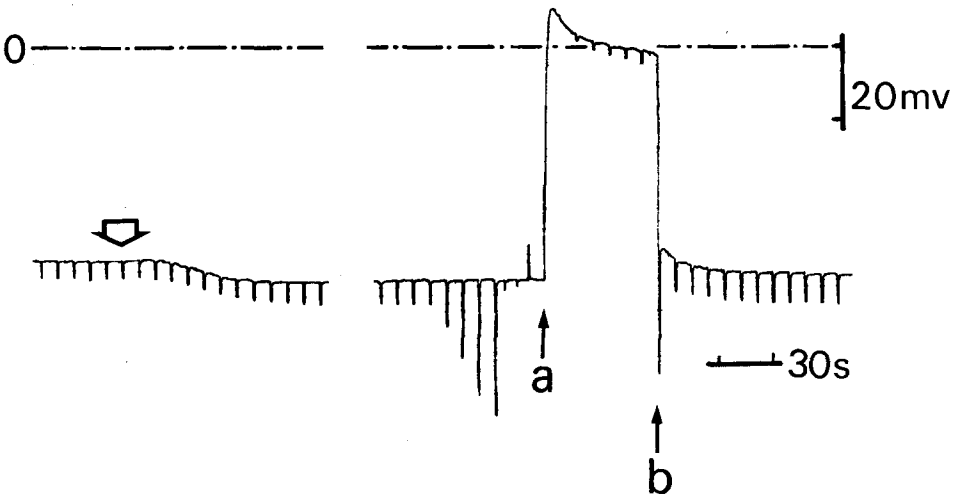

Fig. 1. An all-or-none action potential in Zn-containing saline. Intracellular potential was continuously recorded on a pen-recorder. Hyperpolarizing pulses (1.4 nA, 900 msec) were injected every 9 sec to monitor the input resistance. In four hyperpolarizing pulses before the action potential, the current intensities of the pulses were increased stepwise to demonstrate passive membrane properties. At the open arrow, solution was changed from $MgCl_2$ 24 saline (No. 2 in Table 1) to $ZnCl_2$ 24 saline (No. 3 in Table 1). At steady state in 5 min, depolarizing pulses (2.8 nA, 900 msec) elicited an action potential (arrow at *a*). During the plateau, hyperpolarizing pulses (1.4 nA, 900 msec) were injected to demonstrate membrane resistance decrease. At the 6th pulse of 14 nA, the plateau was abolished (arrow at *b*). Broken line at 0 indicates the reference potential. Omitted part in the record is about 4 min

The possible contribution to this action potential by Ca ions which could remain around the cell was excluded by the following experiment. After two glass microelectrodes had been inserted into the cell in $MgCl_2$ 24 saline (No. 2 in Table 1), the preparation was perfused with EGTA 10 saline (No. 4 in Table 1) to chelate remaining Ca ions. During this perfusion, the resting membrane potential decreased from -58 to -49 mV and input resistance decreased to about 30% (1.64 MΩ) of that in the $MgCl_2$ 24 saline. After 5 min, extracellular saline was changed to experimental ZnF_2 24 saline containing Ca ions at concentration as low as 10^{-8} M (No. 10 in Table 1), here the resting membrane potential increased to -63 mV and the input resistance increased to 115% (6.3 MΩ) as compared with those in $MgCl_2$ 24 saline.

With a depolarizing stimulus (upward arrow in Fig. 2A), an all-or-none action potential was elicited. The threshold potential of this action potential was about -40 mV (oblique arrow in *B*1) and the peak of the action potential was $+10$ mV. MRR, indicating the maximum inward

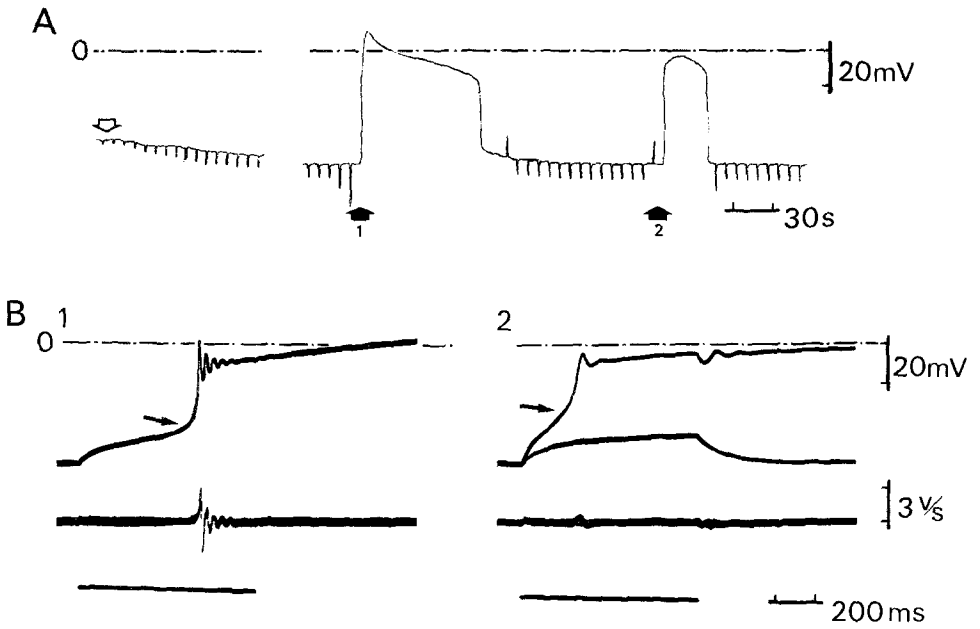

Fig. 2. Action potentials in ZnF_2 saline. (*A*): Pen-record trace. After chelating remaining Ca ions in EGTA 10 saline (No. 4 in Table 1), the solution was changed at open arrow to ZnF_2 24 saline (No. 10 in Table 1), extracellular Ca ion concentration being as low as 10^{-8} M. At steady state in 8 min, depolarizing pulse (1.4 nA, 900 msec) elicited an action potential lasting about 100 sec (upward arrow *1*). After 120 sec interval, a second action potential was evoked but its amplitude and duration were reduced (upward arrow *2*). During the resting state, hyperpolarizing pulses (1.4 nA, 900 msec) were injected every 9 sec to monitor the input resistance. Broken line at 0 indicates the reference potential. Omitted part in record is about 5 min. (*B*): Oscilloscope traces of the action potentials shown in *A*; *B*1 and *B*2 correspond to the first and the second action potentials, respectively. In each figure, upper trace is membrane potentials and lower is their time differentiation with an electronic circuit. Horizontal bar below shows duration of stimuli (intensity, 1.4 nA in *B*1, 1.4 and 2.8 nA in *B*2). Broken line at 0 indicates the reference potential. Oblique arrow indicates the threshold membrane potential

current during the action potential, was 2.9 V/sec (second trace in *B*1). After the peak of the action potential, plateau-like depolarization continued for 90 to 120 sec and repolarized slowly. When the membrane potential reached between -13 and -16 mV, it began to repolarize rather rapidly to the previous resting membrane potential, and in most cases was succeeded by a small after-depolarization. At the peak of the action potential the membrane resistance, measured with hyperpolarizing pulses of 1.4 nA (duration 900 msec) injected into the cell, was reduced to 1/10 as compared with the resting state. In the course of the after-depolarization, the membrane resistance increased by 5 to 15%.

These features of the action potential in Ca-buffered saline are almost the same as those obtained in $ZnCl_2$ saline. It can be safely concluded that these action potentials were due to extracellular Zn ions but not due to residual Ca ions. These action potentials are named *Zn-potentials* hereafter.

After generation of a Zn-potential, the membrane excitability decreased; the second Zn-potential, evoked with a 120-sec interval, became shorter in its duration (30 to 40 sec) and smaller both in its peak potential (−5 to 0 mV) and in its MRR (0.65 V/sec) (Fig. 2*A* and *B*2). This decrease in the membrane excitability did not recover even with a 30-min interval, and therefore it is not like the ordinary refractory period which follows Na and Ca action potentials. It is probably due to a secondary effect of those Zn ions which have permeated the membrane during the preceding Zn-potential. A similar but a smaller excitability decrease has been reported also in Mn-dependent action potentials in guinea pig heart muscle (Ochi, 1976) and Ba-dependent action potentials in barnacle muscle fiber (Hagiwara & Naka, 1964).

It was noted, however, that if the preceding Zn-potential had been abolished at about 5 sec from onset with a hyperpolarizing current pulse (18 nA, 900 msec), the decrese in membrane excitability became less prominent; at the 6th Zn-potential, decrease in the peak membrane potential was less than 4 mV. Decrease in MRR was also smaller; at the 4th Zn-potential it decreased to 80 to 68% of its control value. Whenever it was necessary to record several Zn-potentials from the same cell, this abolishing method was used.

Dependence on External Zn Concentrations

In order to test the dependence of Zn-potential on external Zn concentrations, it was necessary to minimize the possible contribution of K permeability which is known to increase during depolarization (Hodgkin & Huxley, 1952; Neher & Lux, 1972; Kostyuk, Krishtal & Doroshenko, 1975*a*). For this purpose, 50 mM TEA^+ (tetraethyl ammonium ion) was added to experimental salines Zn concentration of which were varied from 3 to 24 mM (No. 11 to 14 salines in Table 1). Extracellular TEA^+ concentration of 50 mM has been shown to be enough to suppress delayed K permeability as well as transient early K permeability in snail neurons (Neher & Lux, 1972; Kostyuk, Krishtal and Doroshenko, 1975*b*). Hence, the MRRs and peak levels of the Zn-potentials evoked in these salines can be assumed to reflect the Zn permeability of the membrane in a straightforward way.

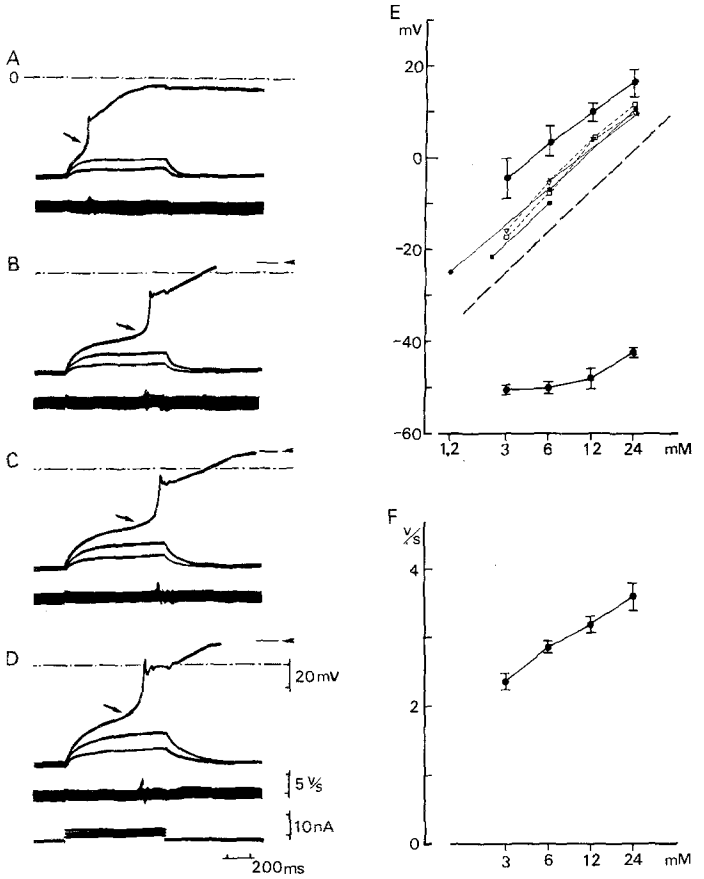

Fig. 3. Dependence of Zn-potentials on external Zn-concentrations. (*A*) to (*D*): Typical oscilloscope traces of Zn-potentials from one neurone in various Zn concentrations in the presence of 50 mM TEA; Zn concentrations were 3 mM in *A* (No. 11 saline in Table 1), 6 mM in *B* (No. 12), 12 mM in *C* (No. 13), and 24 mM in *D* (No. 14). In each figure, upper trace is membrane potential and lower is its time differentiation. Broken line indicates the reference potential. Oblique arrow indicates the threshold membrane potential. Lowermost trace in *D* indicates injected currents common to *A–D* (intensities, 1.4, 2.8, and 4.2 nA). In *B–D*, peak levels of Zn-potentials were read from the next frame of a recording film and illustrated by horizontal bars with wedges. In this cell, resting membrane potentials were held at −82 mV by hyperpolarizing DC current (2.3 nA). (*E*): Similar experiments as those of *A–D* were carried out and their peak levels of Zn-potentials (upper in *E*) and the threshold membrane potentials (lower in *E*) are plotted on the average against Zn concentrations. Bars are SD ($n=4$). For comparison, Zn-potentials were obtained in the absence of TEA and their peak levels plotted with small symbols; same symbols indicate same cell. Filled symbols are obtained in $ZnCl_2$ saline such as No. 3 in Table 1 and open ones in ZnF_2 saline such as No. 10 in Table 1. Thick dashed line indicates the Nernstian slope for a Zn electrode; 29 mV/decade. (*F*): The MRRs of the same Zn-potentials in E are plotted against Zn concentration ($n=4$)

As the extracellular Zn ion concentrations varied from 3 mM, through 6 and 12 mM, up to 24 mM in the presence of 50 mM TEA^+, the peak level of Zn-potential increased from −4.7 mV through 3.5 and 10.2 mV, up to 16.8 mV, respectively (Fig. 3*A–D*). This increase of the peak levels approximately followed the Nernstian slope for a Zn electrode (29 mV/decade; dashed line, Fig. 3 *E*). As the external Zn ion concentration was raised, the resting membrane potential was not altered significantly but a larger threshold depolarization was needed for evoking Zn-potentials, as shown by Fig. 3*E* (lower curve). This shift is probably due to a stabilizing action of Zn ions on the negative surface potential of the membrane (Hagiwara & Takahashi, 1967).

As mentioned above, even in a constant extracellular solution the MRRs of Zn-potentials decreased gradually when repetitively evoked by the abolishing method. To minimize this factor, two sets of experiments were carried out with increasing ZnF_2 concentration as from 3 to 24 mM (Fig. 3*A–D*), and another two sets of experiments with decreasing ZnF_2 concentration as from 24 to 3 mM. Mean values of the MRRs of Zn-potentials thus obtained are plotted in Fig. 3*F* together with their standard deviations. As Zn ion concentration increased from 3 through 6 and 12 mM, up to 24 mM, MRRs which indicate the maximum inward current flow during Zn-potentials also increased from 2.3 V/sec through 2.9 and 3.2 V/sec, up to 3.6 V/sec, respectively. These results indicate that, during Zn-potentials, the membrane permeability to Zn ions increases so that the membrane behaves like a Zn electrode.

For comparison, peak levels of Zn-potentials in the absence of TEA^+ were measured in various Zn ion concentrations and plotted with small symbols in Fig. 3*E*. These peak levels are smaller than those obtained in the presence of 50 mM TEA^+. Nevertheless, they fall along a straight line, the slope of which is almost the same as a theoretical one (29 mV/decade).

Though effects of Zn ions on K permeability were not investigated in detail, Zn ions, like TEA^+, probably exert a suppressing effect of K permeability as reported in frog skeletal muscle (Stanfield, 1975). This may explain why the peaks of Zn-potentials changed like Zn electrode even in the absence of TEA^+.

Inhibition of Zn-Potential by La^{3+}, Co^{2+} and Verapamil

As mentioned above, the present preparation has both Ca channels and Na channels in its cell membranes. To determine which of the

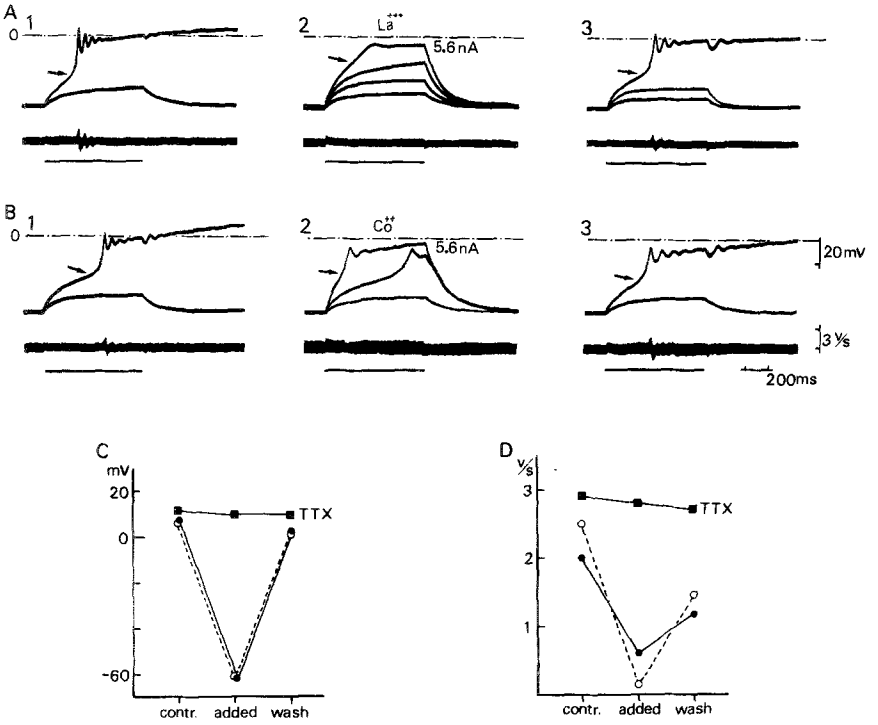

Fig. 4. Effects of TTX, La^{3+} and Co^{2+} on Zn-potentials. (*A*): Effect of 1 mM La^{3+} on Zn-potential. In *A*1, Zn-potential was elicited in normal ZnF_2 24 saline (No. 10 in Table 1), then extracellular solution was changed to a test saline containing 1 mM La^{3+} added to $ZnCl_2$ 24 saline (No. 3 in Table 1). In the test saline (*A*2), Zn-potential was reduced. 8 min after changing back to normal ZnF_2 24 saline, Zn-potential recovered (*A*3). (*B*): Effect of 10 mM Co^{2+} on Zn-potential. Same as in *A* but a test saline in *B*2 contained 10 mM Co^{2+} and 24 mM ZnF_2 (No. 15 in Table 1). Calibrations in *B*3 are common to all traces. Symbols for the reference potential, threshold membrane potential, and stimulus duration are same as in Fig. 2*B*. Stimulus intensities were 1.4 nA steps except the maximum stimuli in *A*2 (5.6 nA) and *B*2 (5.6 nA). (C)–(D): Comparison among the effects of TTX, La^{3+} and Co^{2+} on Zn-potentials. Abscissae indicate conditions of external salines; *contr.* means control saline, *added* means inhibitor-added saline, and *wash* means washing with control saline. Ordinate in *C* indicates amplitudes of Zn-potentials measured 2 sec after their onsets; these values correspond to the peak levels if Zn-potentials form plateaus. Ordinates in *D* show the MRRs of Zn-potentials. Data are obtained from *A* (open circles; effect of 1 mM La^{3+}), from *B* (filled circles; effect of 10 mM Co^{2+}) and from a not-illustrated experiment with 30 μM TTX containing saline (filled squares); TTX was added to No. 10 saline in Table 1

two channels Zn ion permeate, the sensitivity of Zn-potentials to some inhibitors specific to each ionic channel was tested. Tetrodotoxin (TTX) is a specific inhibitor for Na channels (Narahashi, Moore & Scott, 1964);

30 μM of TTX is enough to block Na channels in snail neurone (Lee, Akaike & Brown, 1977, 1978). Even when a high dose of TTX (30 μM) was added to ZnF_2 saline, Zn-potentials showed no significant changes in either the peak level or the MRR (solid squares in Fig. 4*C* and *D*).

By contrast, Co^{2+} or La^{3+} ions which are specific inhibitors for Ca channels (Hagiwara & Takahashi, 1967; Akaike *et al.*, 1978), influenced Zn-potentials appreciably. When 10 mM Co^{2+} ions were added to ZnF_2 24 saline, the MRR of Zn-potential was reduced to 27% of its initial value and the plateau-like depolarization disappeared. The threshold potential shifted in the depolarizing direction by 3 mV. These suppressing actions of Co^{2+} were partially reversible; the MRR recovered in the normal ZnF_2 24 saline was 53% of its initial value. 1 mM La^{3+} was added to $ZnCl_2$ 24 saline instead of ZnF_2 24 saline because in the presence of fluoride La^{3+} forms LaF_3 and precipitates. In the La^{3+} added saline, Zn-potentials were greatly suppressed and produced only a small peak at the onset (Fig. 4*A*2). The MRR decreased to 7% of its initial value. The threshold potential shifted to the depolarizing direction by 12 mV. These suppressing actions of La^{3+} were partially reversible; the MRR of recovered Zn-potentials was 57% of the control value.

When Verapamil, an organic inhibitor for Ca channels, was added to external ZnF_2 24 saline, MRRs of Zn-potentials were reduced (Fig. 5); at the concentration of 3 to 6×10^{-5} g/ml, the MRRs were 50% of the control value (Fig. 5*E*). Verapamil showed no significant effect on the threshold membrane potential (oblique arrows in Fig. 5*A–D*). This contrasts to the cases of Co^{2+} or La^{3+} and indicates that Verapamil has no stabilizing effect on the membrane. The reduction of Zn-potentials by Verapamil did not recover even at more than 10 min after the cell was washed by Verapamil-free saline.

As control, blocking effect of Verapamil on Ca-dependent action potentials was examined. In Fig. 5*E* (open circles), MRRs of Ca-dependent action potentials evoked in $CaCl_2$ 10 saline (No. 5 in Table 1) were plotted against Verapamil concentration. It is concluded that both Zn-potentials and Ca-dependent action potentials were blocked with similar doses of Verapamil, i.e., 10^{-4} g/ml $= 2.21 \times 10^{-4}$ M.

Comparable doses of Verapamil have been used in snail neurons for blocking Ca channels; e.g., 5×10^{-4} M by Kostyuk and Krishtal (1977*b*) and 3×10^{-5} M by Akaike *et al.* (1978).

These results mean that Zn-potentials are generated by Zn ions permeating Ca channels, but that they are not related to Na channels.

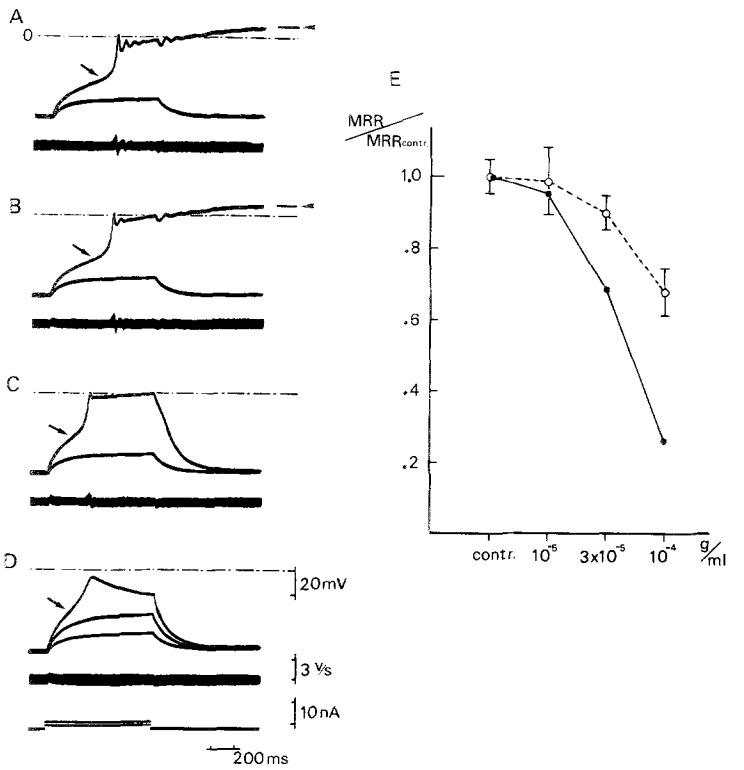

Fig. 5. Effects of Verapamil on Zn potentials. As Verapamil concentration is raised from zero (*A*) through 10^{-5} g/ml (*B*) and 3×10^{-5} g/ml (*C*) up to 10^{-4} g/ml (*D*), Zn-potentials evoked in ZnF_2 24 salines (No. 10 in Table 1) were reduced. Meanings of symbols are same as in Fig. 3*A–D*. In *E*, these MRRs are plotted against Verapamil concentrations after normalization to the control value (1.8 V/sec obtained in *A*). For comparison, effects of Verapamil on Ca-dependent action potentials were examined in $CaCl_2$ 10 salines (No. 5 in Table 1) with increasing doses of Verapamil. The obtained MRRs of the action potentials in these salines are normalized to the control value (28.2 V/sec) and plotted against added Verapamil concentrations with open circles (mean value) and bars (SD, $n=3$)

Effect of Zn Ions on Ca-Dependent Action Potentials

Finally, inhibitory effects on Zn ions on Ca-dependent action potentials were investigated. In the case of Fig. 6, after insertion of two glass microelectrodes in $MgCl_2$ 24 saline, extracellular solution was changed to $CaCl_2$ 10 saline (No. 5 in Table 1). The resting membrane potential was about -59 mV, and when membrane potential was depolarized up to -45 mV, a Ca-dependent action potential was elicited (Fig. 6*A*).

As the external Zn ion concentration was increased to 3, 6, 12, and 24 mM while the Ca ion concentration was held at 10 mM, the peak

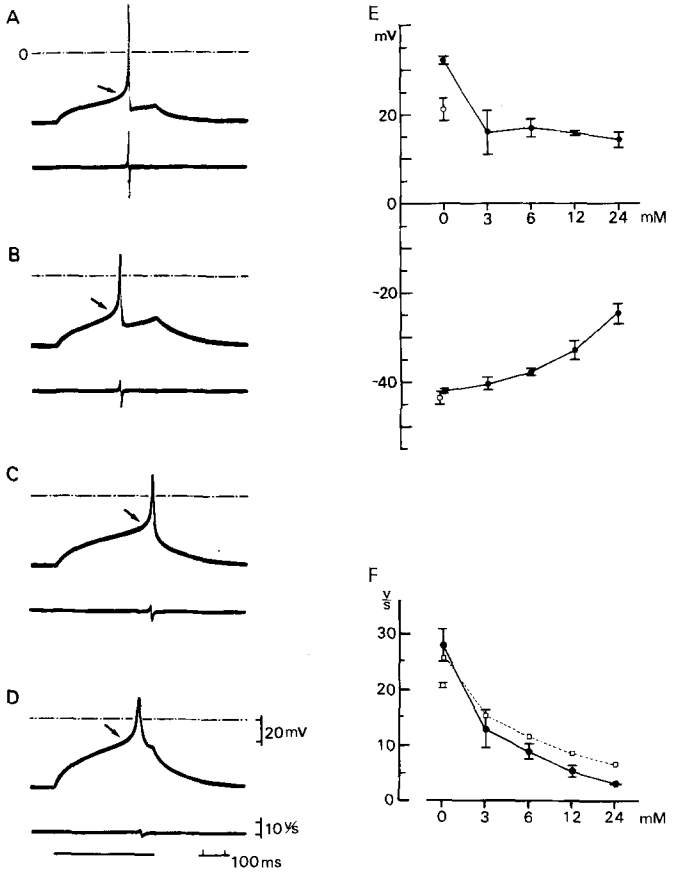

Fig. 6. Effects of Zn ions on Ca-dependent action potentials. Action potentials were evoked from one cell in salines containing 10 mM Ca ions and 0 to 24 mM Zn ions (No. 5 to 9 salines in Table 1). (*A*)–(*D*): Typical records of these action potentials; Zn ion concentrations are 0 mM (*A*), 6 mM (*B*), 12 mM (*C*) and 24 mM (*D*). Upper trace is the membrane potential and lower trace is its time differentiation. Broken line indicates the reference potential. Oblique arrow indicates the threshold potential. Horizontal bar below *D* indicates duration of stimuli (450 msec); their intensities were 1.9 nA (*A*), 1.9 nA (*B*), 2.2 nA (*C*), and 3.3 nA (*D*). (*E*): Plots of the peak levels (upper in *E*) and the threshold membrane potentials (lower in *E*) of these action potentials against Zn ion concentrations. Filled circles are mean values and bars are SD ($n=3$). Open circles are values obtained 8 min after washing in control saline (No. 5 in Table 1). (*F*): The MRRs of these action potentials are plotted in a similar manner as in *E*. Open squares are calculated values of MRRs on assumptions mentioned in the text

levels of action potentials were reduced from 32 mV of control to 16, 17, 16, and 14 mV, respectively (Fig. 6*E*). Simultaneously, the duration of the action potential was prolonged and the maximum rate of fall of the action potential was reduced (Fig. 6*B–D*) probably due to suppres-

sion or decrease of repolarizing ionic mechanisms in the membrane such as delayed K permeability and/or Ca-induced K permeability (Meech, 1974). The MRRs of these action potentials were reduced from 28 V/sec of control to 13, 9, 5.5, and 3 V/sec, respectively (Fig. 6*F*). The decrease of MRRs can be explained by assuming that Zn ions compete with Ca ions in binding to the "sites" of Ca channels (*see Discussion*); values of MRRs calculated on this assumption are plotted in Fig. 6*E* (open squares). These inhibitory effects of Zn were reversible; data obtained 8 min after washing in the normal $CaCl_2$ 10 saline were also plotted in Fig. 6*E* and *F* (open circles).

Discussion

In molluscan nerve cells, all-or-none action potentials of long duration were elicited in Na-free salines even after extracellular Ca ions were totally replaced with Zn ions. The amplitudes and MRRs of these action potentials depended on external Zn ion concentrations. During these action potentials, the membrane conductance increased. Therfore, it is concluded that these are Zn-potentials generated by the increase of membrane permeability to external Zn ions. Zn-potentials are suppressed by Co^{2+}, La^{3+} or Verapamil which are specific inhibitors for Ca channels, whereas no significant change in Zn-potential occurs even with a high dose of TTX which is a specific inhibitor for Na channels. It is evident that Zn-potentials are generated by Zn ions permeating Ca channels in the membrane and that they have no relevance to Na channels.

Concerning the mechanisms for divalent cations to permeate Ca channels, Hagiwara and Takahashi (1967) have presented a simple model consisting of two steps. The first step is a reversible binding of external divalent cations to "sites" of the membrane with a dissociation constant K_x. Each "site" belongs to each Ca channel in the membrane and their total number is finite. The second step is permeation of the bound divalent cations through the pore structure of Ca channels in the membrane. With this model the following relationship between the concentration of external divalent cation $[X]$ and MRR of its action potential is formulated.

$$\frac{\mathrm{MRR}_{\max}}{\mathrm{MRR}} = 1 + \frac{K_x}{[X]} \tag{1}$$

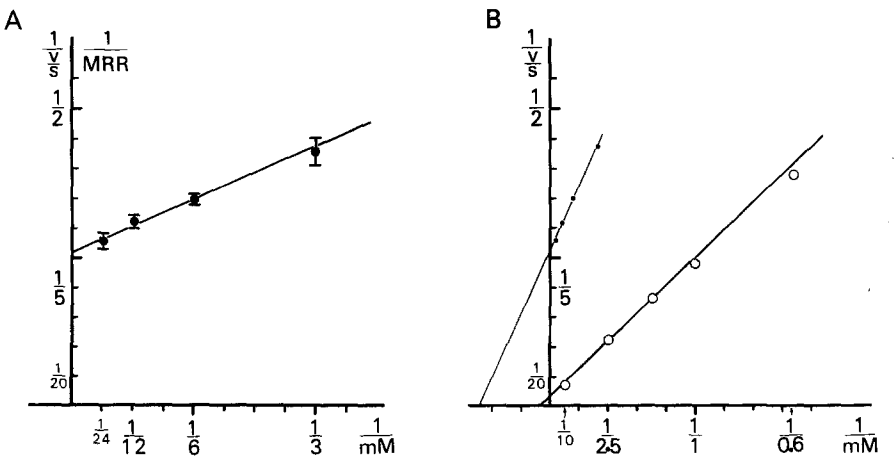

Fig. 7. Analysis of maximum rate of rise according to a model. (*A*): Reciprocals of MRRs of Zn-potentials (Fig. 3*F*) were plotted against reciprocals of Zn concentrations. Solid circles are average values. Bars are SD ($n=4$). Data nearly fall on a straight line which intersects with X axis and Y axis around $-1/2.10$ mM and 1/3.9 V/sec, respectively (*See* text for theoretical interpretation.) (*B*): Similar plot as in *A* for Cadependent action potentials obtained from one cell in various concentrations of Ca ions; i.e., 0.6, 1, 1.43, 2.5, and 10 mM Ca ions. Data nearly fall on a straight line which intersects with X axis and Y axis around $-1/13$ mM and 1/61 V/sec, respectively. For comparison, average values in *A* are also plotted with small solid circles

where MRR_{max} is MRR obtained when all the sites are occupied with divalent cation X, and K_X is the dissociation constant of the sites for divalent cation X.

The data of MRRs of Zn-potentials obtained in various external Zn concentrations (Fig. 3) were analyzed with this equation; when reciprocals of MRRs were plotted against reciprocals of external Zn concentration (Fig. 7*A*), each point fell along a straight line, conforming to Eq. (1). From the intersections of the line with the X-axis and Y-axis, K_{Zn} was calculated as 2.1 mM and MRR_{max} for Zn ion as 3.9 V/sec. From similar analyses applied to the Ca-dependent action potentials (Fig. 7*B*), K_{Ca} was calculated as 10 to 19 mM (mean 14 mM) and MRR_{max} for Ca ions as 52 to 64 V/sec (mean 59 V/sec). The fact that K_{Zn} is 1/5 to 1/10 of K_{Ca} indicates that Zn ions are 5 to 10 times stronger than Ca ions in their affinity to the sites of Ca channels. That the MRR for Zn ions is 1/10 to 1/20 of that for Ca ions means that Zn ions are 10 to 20 times less mobile through Ca channels than Ca ions.

Inhibitory effects of Zn ions on Ca action potentials (Fig. 6) could be derived from the above model, under the assumption that both Zn ions and Ca ions bind to the sites of Ca channels with respective dissocia-

tion constants, while the total number of the sites remains constant. Figure 6*F* shows that, as the external Zn concentration increases, calculated MRR decreases and fits experimental values reasonably well. As mentioned above, the shift of the threshold membrane potential in the depolarizing direction (lower plots in Fig. 6*E*) caused by higher Zn concentration may be explained as due to changes in the external surface potential (Frankenhauser & Hodgkin, 1957). By taking this factor into consideration, calculated values of MRRs come closer to experimental values.

One puzzling problem, however, is that while the dissociation constant of the sites of Ca channels for Zn ion was estimated as about 2.1 mM, the dependence of the peak levels of Zn-potentials on external Zn ion concentrations did not show appreciable saturation up to 24 mM (Fig. 3*E*). In the present case, one possible explanation is that the Zn-potentials reach their peak levels so slowly, taking 0.6 to 2 sec after the onsets (Fig. 3*A–D*), that the dissociation constant of the site may change during these depolarizations. According to Akaike *et al.* (1978), the dissociation constant of Ca channels in snail neurons increased when the membrane was depolarized, and thus shifted the occurrence of saturation in Ca inward currents to higher Ca concentration. Similar discrepancy was also reported in Ca-dependent action potentials of annelid egg cell; peak potentials changed along the Nernst slope for a Ca electrode up to 100 mM Ca ion concentraion while MRRs deviated from linearity even at $25 \sim 50$ mM (Hagiwara & Miyazaki, 1977*b*). But a further analysis is necessary with a voltage clamp method for solving this problem.

Duration of Zn-potentials is long, several thousand times the duration of Ca action potentials. This leads to a speculation that during Zn-potentials the depolarizing ionic mechanism in the membrane continues for long time, while the repolarizing ionic mechanism in the membrane is reduced or inhibited. The former mechanism corresponds to Zn permeability and the latter to the so-called delayed K permeability. The long-lasting increase of Zn permeability means a slow inactivation of Ca channel. Indeed, Lee *et al.* (1978) revealed a slow inactivation of Ca currents in snail neurons by voltage clamp method combined with intracellular perfusion technique. Inhibitory effects of Zn ions on delayed K permeability were observed in frog skeletal muscle (Stanfield, 1975) and in insect larval muscle (Fukuda & Kawa, 1977). Similar inhibition of K permeability may also occur in the present preparation, for the peak levels of Zn-potentials behave like Zn electrode even in the absence of TEA^+ (small symbols in Fig. 3*E*).

Another feature of Zn-potentials is the decrease of membrane excitability due to previous Zn-potentials. One possible cause for this is decrease of Zn ion concentration gradient across the cell membrane. An approximate estimation that after one Zn-potential Zn ion concentration in the cell increases by about 10^{-7} M is derived from the assumption that the cell is a sphere 200 μm across with specific membrane capacity of 1 μF/cm^2 and generates the Zn-potential of 70 mV in amplitude. Intracellular Zn ion concentration of 10^{-7} M, however, does not seem to be sufficient to reduce the concentration gradient. Another possible cause is the direct effect of Zn ions on the internal surface of the membrane; Zn ions may bind to some structure of the membrane and so block Ca channels. In internally perfused giant axons of squid, intracellular Zn ions actually suppress Na channels by immobilizing the gating molecules (Armstrong & Bezanilla, 1974). In the mossy fiber of mammalian hippocampus, Zn content of these axons is especially high, and some authors speculate that intracellular Zn suppresses the electrical excitability of the axon (Euler, 1962; Crawford, Doller & Connor, 1973).

The fact that Zn ions can permeate Ca channels gives us important suggestions as to molecular mechanisms of Ca channels. As for the ion selectivity of the ion channels in the excitable membrane, geometric relationship between ion radius and pore radius of the channel is one of the key factors (Hille, 1975). Ionic crystal radii of permeant ions such as Ca^{2+} (0.99 Å), Sr^{2+} (1.13 Å), Ba^{2+} (1.35 Å) are larger than crystal radii of Mg^{2+} (0.65 Å), Ni^{2+} (0.70 Å), Co^{2+} (0.72 Å) (Robinson & Stokes, 1959) which are so far considered nonpermeant through Ca channels (Hagiwara & Miyazaki, 1977*a*; Akaike *et al.*, 1978). The ionic radius of Zn^{2+} (0.74 Å) is a little larger than the nonpermeant group. Therefore the lower critical size which limits permeation through Ca channels may exist just below the size of Zn^{2+}. Mn^{2+} (0.80 Å), the crystal radius of which is between Zn^{2+} and Ca^{2+}, has been revealed to permeate the membrane of heart muscle (Delahayes, 1975; Ochi, 1976), Ca channels in insect larval muscle (Fukuda & Kawa, 1977) and Ca channels in tunicate egg cells (Okamoto, Takahashi & Yamashita, 1977). This is also the case in the present snail neuronal membrane (K. Kawa, *unpublished*).

Besides these inferences, the result of this study gives us a new view of the mechanism of facilitatory effect of Zn ions on muscle contraction (Isaacson & Sandow, 1963; Stanfield, 1973) because the sarcolemma was recently revealed to possess Ca channels in addition to the usual Na channels (Stanfield, 1977; Sanchez & Stefani, 1978).

The biological significance of high Zn content in some regions of the mammlian central nervous system (Hassler & Söremark, 1968; Fjerdingstad, Danscher & Fjerdingstad, 1974) remains open to question. Therefore, further investigations into the effect of Zn ions on the present preparation would be meaningful.

This work was carried out as a part of the author's Ph.D. Thesis at the Department of Physiology, Faculty of Medicine, University of Tokyo, Bunkyo-ku, Tokyo, Japan. The author is deeply indebted to Prof. M. Ito, Associate Prof. K. Toyama, and Dr. J. Fukuda for their constant advice and encouragment.

References

Akaike, N., Lee, K.S., Brown, A.M. 1978. The calcium current of *Helix* neuron. *J. Gen. Physiol.* **71**:509

Armstrong, C.M., Bezanilla, F. 1974. Charge movement associated with the opening and closing of the activation gates of the Na channels. *J. Gen. Physiol.* **63**:533

Belton, P., Grundfest, H. 1962. Potassium activation and K spikes in muscle fibers of the mealworm larva (*Tenebrio molitor*). *Am. J. Physiol.* **203**:588

Benoit, P.R., Mambrini, J. 1970. Modification of transmitter release by ions which prolong the presynaptic action potential. *J. Physiol. (London)* **210**:681

Crawford, I.L., Doller, H.J., Connor, J.D. 1973. Diphenylthiocarbazone effects on evoked waves and zinc in the rat hippocampus. *Pharmacologist* **15**:197

Dean, J.A. 1973. Analytical Chemistry. Tables 5–6. *In*: Lange's handbook of chemistry. (11th ed.) J.A. Dean, editor. pp. 5–8. McGraw-Hill, New York

Delahayes, J.F. 1975. Depolarization-induced movement of Mn^{2+} across the cell membrane in the guinea pig myocardium. *Circulation Res.* **36**:713

Euler, C. von 1962. On the significance of the high zinc content in the hippocampal formation. *In*: Physiologie de l'Hippocampe. P. Passouant, editor. p. 135. Editions du C.N.R.S., Paris

Ferroni, A., Blanchi, D. 1965. Maximum rate of depolarization of single muscle fiber in normal and low sodium solutions. *J. Gen. Physiol.* **49**:17

Fjerdingstad, E., Danscher, G., Fjerdingstad, E.J. 1974. Zinc content in hippocampus and whole brain of normal rats. *Brain Res.* **79**:338

Frankenhaeuser, B., Hodgkin, A.L. 1957. The action of calcium on the electrical properties of squid axons. *J. Physiol. (London)* **137**:218

Fukuda, J., Kawa, K. 1977. Permeation of manganese, cadmium, zinc and beryllium through calcium channels of an insect muscle membranes. *Science* **196**:309

Hagiwara, S., Miyazaki, S. 1977*a*. Ca and Na spikes in egg cell membrane. *In:* Cellular Neurobiology. p. 147. Alan R. Liss, New York

Hagiwara, S., Miyazaki, S. 1977*b*. Changes in excitability of the cell membrane during 'differentiation without cleavage' in the egg of the annelid, *Chaetopterus pergamentaceus*. *J. Physiol (London)* **272**:197

Hagiwara, S., Naka, K.I. 1964. The initiation of spike potential in barnacle muscle fibers under low intracellular Ca^{++}. *J. Gen. Physiol.* **48**:141

Hagiwara, S., Takahashi, K. 1967. Surface density of calcium ions and calcium spikes in the barnacle muscle fiber membrane. *J. Gen. Physiol.* **50**:583

Hassler, O., Söremark, R. 1968. Accumulation of zinc in mouse brain. An autoradiographic study with ^{65}Zn. *Arch. Neurol.* **19**:117

Hille, B. 1975. Ionic selectivity of Na and K channels of nerve membranes. *In:* Membranes. A Series of Advances. G. Eisenman, editor. Vol. 3, chap. 4, p. 255. Marcel Dekker, New York

Hodgkin, A.L., Huxley, A.F. 1952. Currents carried by sodium and potassium ions through the membrane of the giant axon of *Loligo*. *J. Physiol. (London)* **116**:449

Isaacson, A., Sandow, A. 1963. Effects of zinc on responses of skeletal muscle. *J. Gen. Physiol.* **46**:655

Katz, B., Miledi, R. 1965. The effect of calcium on acetylcholine release from motor nerve terminals. *Proc. R. Soc. London B.* **161**:496

Kerkut, G.A., Gardner, D.R. 1967. The role of calcium ions in the action potentials of *Helix aspersa* neurones. *Comp. Biochem. Physiol.* **20**:147

Klein, M., Kandel, E. 1978. Presynaptic modulation of voltage-dependent Ca^{2+} current: Mechanism for behavioral sensitization in *Aplysia calfornica*. *Proc. Nat. Acad. Sci. USA* **75**:3512

Kostyuk, P.G., Krishtal, O.A. 1977*a*. Separation of sodium and calcium currents in the somatic membrane of mollusc neurones. *J. Physiol. (London)* **270**:545

Kostyuk, P.G., Krishtal, O.A. 1977*b*. Effects of calcium and calcium-chelating agents on the inward and outward current in the membrane of mollusc neurons. *J. Physiol. (London)* **270**:569

Kostyuk, P.G., Krishtal, O.A., Doroshenko, P.A. 1975*a*. Outward currents in isolated snail neurones: I. Inactivation kinetics. *Comp. Biochem. Physiol.* **51C**:259

Kostyuk, P.G., Krishtal, O.A., Doroshenko, P.A. 1975*b*. Outward currents in isolated snail neurones: II. Effect of TEA. *Comp. Biochem. Physiol.* **51C**:265

Kusano, K., Grundfest, H. 1967. Ionic requirements for synaptic electrogenesis in neuromuscular transmission of mealworm larvae (*Tenebrio molitor*). *J. Gen. Physiol.* **50**:1092

Lee, K.S., Akaike, N., Brown, A.M. 1977. Trypsin inhibits the action of tetrodotoxin on neurones. *Nature (London)* **265**:751

Lee, K.S., Akaike, N., Brown, A.M. 1978. Properties of internally perfused, voltage-clamped, isolated nerve cell bodies. *J. Gen. Physiol.* **71**:489

Meech, R.W. 1974. The sensitivity of *Helix aspersa* neurones to injected calcium ions. *J. Physiol. (London)* **237**:259

Miledi, R. 1966. Strontium as a substitute for calcium in the process of transmitter release at the neuromuscular junction. *Nature (London)* **212**:1233

Miyazaki, S., Ohmori, H., Sasaki, S. 1975. Action potential and non-linear current-voltage relation in starfish oocytes. *J. Physiol. (London)* **246**:37

Murayama, K., Lakshminarayanaiah, N. 1977. Some electrical properties of the membrane of the barnacle muscle fibers under internal perfusion. *J. Membrane Biol.* **35**:257

Narahashi, T., Moore, J.W., Scott, W.R. 1964. Tetrodotoxin blockage of sodium conductance increase in lobster giant axons. *J. Gen. Physiol.* **47**:965

Neher, E., Lux, H.D. 1972. Differential action of TEA^+ on two K^+-current components of a molluscan neurone. *Pfluegers Arch.* **336**:87

Ochi, R. 1976. Manganese-dependent propagated action potentials and their depression by electrical stimulation in guinea-pig myocardium perfused by sodium-free media. *J. Physiol. (London)* **263**:139

Okamoto, H., Takahashi, K., Yamashita, N. 1977. Ionic currents through the membrane of the mammalian oocyte and their comparison with those in the tunicate and sea urchin. *J. Physiol. (London)* **267**:465

Robinson, R.A., Stokes, R.H. 1959. Appendix 3.1, Table of ionic radii. *In:* Electrolyte Solutions. p. 461. Butterworth, London

Sanchez, J.A., Stefani, E. 1978. Inward calcium current in twitch muscle fibres of the frog. *J. Physiol. (London)* **283**:197

Sandow, A., Bien, S.M. 1962. Blockade of neuromuscular transmission by zinc. *Nature (London)* **193**:689

Standen, N.B. 1975*a*. Calcium and sodium ions as charge carriers in the action potential of an identified snail neurone. *J. Physiol. (London)* **249**:241

Standen, N.B. 1975*b*. Voltage-clamp studies of the calcium inward current in an identified snail neurone: Comparison with the sodium inward current. *J. Physiol. (London)* **249**:253

Stanfield, P.R. 1973. The onset of the effects of zinc and tetraethylammonium ions on action potential duration and twitch amplitude of single muscle fibres. *J. Physiol. (London)* **235**:639

Stanfield, P.R. 1975. The effect of zinc ions on the gating of the delayed potassium conductance of frog sartorius muscle *J. Physiol. (London)* **251**:711

Stanfield, P.R. 1977. A calcium dependent inward current in frog skeletal muscle fibres. *Pfluegers Arch.* **368**:267

Sugaya, A., Sugaya, E., Tsujitani, M. 1973. Pentylenetetrazol-induced intracellular potential changes of the neuron of the Japanese land snail *Euhadra peliomphala*. *Jpn. J. Physiol.* **23**:261

Wald, F. 1972. Ionic differences between somatic and axonal action potential in snail giant neurones. *J. Physiol. (London)* **220**:267